ASIAN JOURNAL OF CIVIL ENGINEERING (BHRC) VOL. 16, NO. 6 (2015)
PAGES 733-750

EFFECT OF MATERIAL DETERIORATION ON THE SEISMIC COLLAPSE CAPACITY OF P-DELTA VULNERABLE SDOF SYSTEMS

D. Kampenhuber and C. Adam*
Unit of Applied Mechanics, University of Innsbruck, Innsbruck, Austria

Received: 18 February 2015; **Accepted:** 20 April 2015

ABSTRACT

The aim of the present contribution is quantify the effect of material deterioration on the seismic collapse capacity of single-degree-of-freedom systems vulnerable to the destabilizing effect of gravity loads (P-delta effect). The outcomes are presented in terms of collapse capacity spectra, where for characteristic structural parameters median and dispersion of record-dependent collapse capacities is plotted against the initial structural period. The ultimate goal of this study is to isolate sets of material deterioration parameters, which do not affect substantially the collapse capacity of P-delta sensitive structures. These threshold values depend primarily on the post-yield stiffness ratio, the assigned hysteretic law, and the initial structural period.

Keywords: Collapse capacity spectrum; dynamic instability; P-delta effect; material deterioration; record-to-record variability; seismic excitation.

1. INTRODUCTION

Sidesway collapse of a structural building subjected to severe earthquake excitation is the consequence of successive reduction of the lateral load carrying capacity resulting from stiffness and strength deterioration, and the global destabilizing effect of gravity loads acting through lateral displacements (P-delta effect) [1]. Depending on the structural configuration and earthquake characteristics one of these effects may be primarily responsible for this type of structural failure. In very flexible buildings the destabilizing effect of gravity loads may lead to a negative post-yield stiffness, and as a consequence, the structural collapse capacity might be exhausted at a rapid rate when the earthquake drives the structure into its inelastic range of deformation, even for stable hysteretic component behavior [2]. In many other buildings the destabilizing effect of gravity loads is negligible, and structural collapse is a result of material deterioration only. Cyclic material deterioration depends also on the loading

*E-mail address of the corresponding author: christoph.adam@uibk.ac.at (C. Adam)

history: when an earthquake induces only very few inelastic cycles, this effect is not of significance for seismic collapse of most of the structures [3, 4]. In contrast, long lasting, almost harmonic earthquakes may facilitate distinct material deterioration [5]. Adam and Jäger [6, 7] have studied rigorously the collapse capacity of highly inelastic P-delta sensitive single-degree-of-freedom (SDOF) systems with non-deteriorating cyclic behavior. Based on a set of representative ground motions, collapse capacity spectra have been derived, which quantify the collapse capacity as a function of the initial period, the negative post-yield stiffness ratio, and the viscous damping coefficient. These spectra are the basis of the collapse capacity spectrum methodology that allows seismic collapse assessment of P-delta sensitive regular frame structures with simple measures [8]. However, in reality P-delta induced collapse comes to a certain extent always along with material deterioration. Thus, the aim of the present contribution is to quantify the effect of combined strength and stiffness deterioration on collapse capacity spectra. The ultimate goal is to isolate sets of material deterioration parameters that do not affect substantially the collapse capacity of P-delta sensitive structures.

2. DEFINITIONS AND FRAMEWORK

2.1 Underlying mechanical model

The collapse capacity of an SDOF system considering the effects of gravity loads and material deterioration is studied, utilizing the mechanical model of an inverted mathematical pendulum with a lumped mass *m* at it the tip of the rigid rod, as shown in Fig. 1. The rod of length *h* is simply supported, and the elastic and inelastic properties of the system are assigned to a rotational elastic-plastic spring at the base. k_r denotes the initial rotational spring stiffness. A rotational viscous dashpot damper is connected in parallel to the spring. The tip of the system is subjected to gravity load *P*, inducing a geometric nonlinear response due to the P-delta effect. Horizontal seismic acceleration $\ddot{x}_g$ at the base excites the system to vibrations. In [9] it has been shown that seismic induced structural collapse of realistic buildings occurs before effects of large deformations become important. Consequently, in the present study the geometric linearized rotation φ (i.e., $|\varphi| << 1$) normalized with respect to the corresponding quantity at yield, φ_y, represents the engineering demand parameter (EDP) $\mu (= \varphi / \varphi_y)$.

2.2 Inelastic material modeling

The modified Ibarra-Medina-Krawinkler model [3] is used for nonlinear constitutive modeling. This model requires the definition of

- a backbone curve,
- a basic hysteretic model, whose characteristic parameters such as strength and yield displacement are calibrated to corresponding quantities of the backbone curve, and
- a model that controls stiffness and strength deterioration.

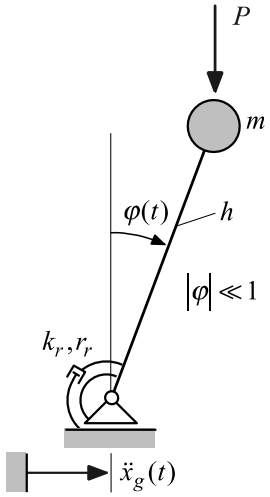

Figure 1. Mechanical model of the considered SDOF system vulnerable to P-delta (Ref. [6])

In the present investigation a bilinear backbone curve with hardening ratio α is assigned to the rotational spring of the SDOF system. I.e., post-capping strength deterioration of structural component is not considered.

The standard *bilinear model* (Fig. 2a) with kinematic hardening and the *peak-oriented model* (Fig. 2b) describe two different types of basic hysteretic cyclic system behavior. Details on these hysteretic models are found in [3], [10], [11], and [12]. The effect of *pinching* hysteretic behavior is not studied separately, because in [6] and [13] it has been confirmed that the corresponding seismic response is of the same magnitude as if a *peak-oriented* hysteretic model is assigned to the system [14].

In the modified Ibarra-Medina-Krawinkler model the dissipated hysteretic energy is the prime parameter for cyclic stiffness and strength deterioration, expressed in terms of the variable $\beta_{k,i}$ [11],

$$\beta_{k,i} = \left(\frac{E_i}{E_{t,k} - \sum_{j=1}^{i} E_j} \right)^{c_k} D^{+/-} \tag{1}$$

Parameter D defines the decrease of the cyclic deterioration rate in the positive (D^+) or negative (D^-) loading direction, and can only be $D^{+/-} \leq 1$. If the rate of cyclic deterioration is the same in both loading directions, then $D^{+/-} = 1$. E_i represents the hysteretic energy dissipated in the *i*th inelastic excursion (see e.g. E_1 in Fig. 2c), and $\sum_j E_j$ is the hysteretic energy dissipated in all previous excursions through loading in both positive and negative direction (i.e., $E_1 + E_2$ for the example of Fig. 2c).

The hysteretic energy dissipation capacity for the cyclic deterioration mode "*k*",

$$E_{t,k} = \Lambda_k M_{sy} \tag{2}$$

is mostly controlled by parameter Λ_k [4]. In Eqs (1) and (2) index "*k*" denotes the considered cyclic deterioration mode. Experimental studies have revealed that in general it should be distinguished between

- the basic strength deterioration mode (i.e., $k = S$),
- the post-capping strength deterioration mode (i.e., $k = C$)
- the unloading stiffness deterioration mode (i.e., $k = K$), and
- the reloading stiffness deterioration mode (i.e., $k = A$).

Consequently, parameter Λ_k of Eq. (2) can be defined independently for each of these deterioration modes, then denoted as Λ_S, Λ_C, Λ_K, and Λ_A, respectively. For practical applications these parameters are calibrated from outcomes of experimental investigations. Note that in this study the post-capping strength deterioration mode does not exist since the backbone curve is purely bilinear. The reloading stiffness deterioration is only present in peak-oriented cyclic behavior. Exponent c_k $(1.0 \le c_k \le 2.0)$ of Eq. (1) controls the rate of deterioration of the evaluated deterioration mode, and can also be defined for each deterioration mode "*k*" separately. $c_k = 1$ implies a constant rate of deterioration [12].

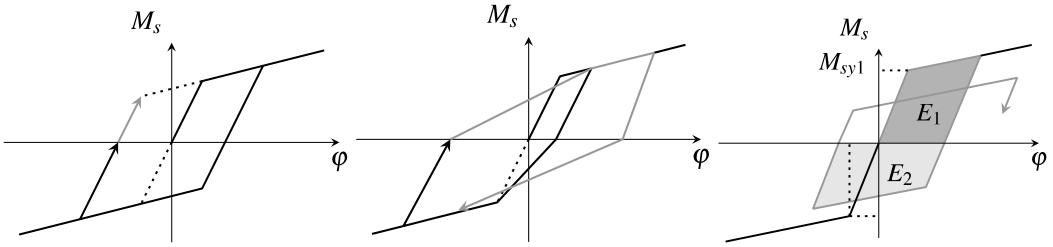

Figure 2. (a) Bilinear hysteretic model. (b) Peak-oriented hysteretic model. (c) Bilinear hysteretic model with strength deterioration

For instance, basic strength deterioration in the *i*th inelastic excursion is governed by

$$M^{+}_{sy,i} = \left(1 - \beta_{S,i}\right) M^{+}_{sy,i-1} \tag{3}$$

Where $M^{+}_{sy,i}$ represents the deteriorated yield strength of the rotational spring after the *i*th excursion, and $M^{+}_{sy,i-1}$ is the deteriorated yield strength before this excursion. $\beta_{S,i}$ denotes the corresponding yield strength deterioration coefficient according to Eq. (1). A positive and a negative value can be defined for each deterioration parameter, because in general each parameter may deteriorate independently in tension and compression [11]. In

the present study, however, parameter deterioration is coupled in tension and compression. [11], [12] and [3] provide detailed explanations about this constitutive deterioration model.

2.3 P-Delta effect on an inelastic SDOF system

In an SDOF system as shown in Fig. 1a the stability coefficient θ [6],

$$\theta = \frac{Ph}{k_r} \tag{4}$$

Controls the P-delta effect [15]. The gravity load P leads to a shear deformation of the normalized hysteretic force-displacement relationship, because the normalized system force $\overline{f}$ is reduced by $\theta\mu$ while the corresponding normalized system deformation μ remains unaffected [15]. In Fig. 3 this situation is shown for a single load cycle of an SDOF system with bilinear hysteretic loop. If the stability coefficient θ exceeds the hardening coefficient α (i.e. $\theta > \alpha$), the post-yield stiffness is negative, and consequently the SDOF system is prone to seismic induced collapse, even if component deterioration is omitted [6].

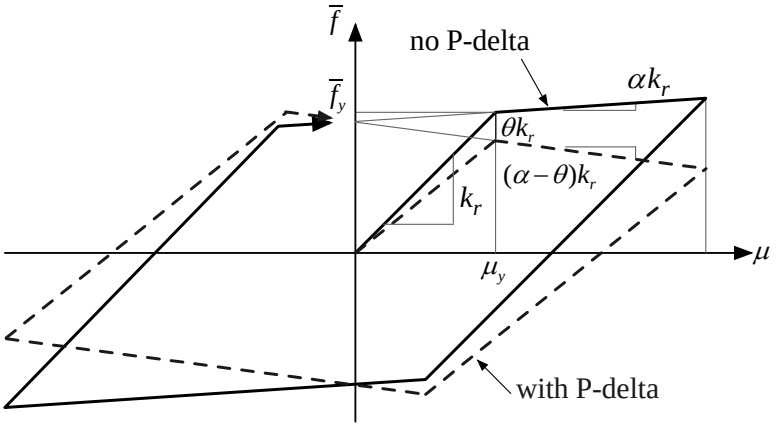

Figure 3. Bilinear hysteretic behavior of a non-deteriorating P-delta vulnerable SDOF system for a single load cycle disregarding and considering P-delta (after [6])

2.4 Characteristic structural parameters for collapse

In [6, 13] it is shown that P-delta induced collapse of a non-deteriorating SDOF system with a bilinear backbone curve, subjected to a specific ground motion record, is governed by the following characteristic structural parameters:

- Initial structural period *T*
- Viscous damping coefficient ζ
- Negative post-yield stiffness ratio, expressed by the difference of the stability coefficient and the hardening ratio $\theta - \alpha$ (>0)
- Hysteretic model

If component deterioration as described before is taken into account, additionally

deterioration parameters Λ_S, Λ_A, Λ_K, c_S, c_A and c_K must be defined, compare with Eqs (1) and (2). In the present study the effect of *no*, *slow*, *medium*, and *rapid* combined stiffness and strength deterioration as defined in [11] on collapse is assessed. The corresponding parameters are listed in Table 1. In the numerical study the initial (elastic) structural period *T* (disregarding P-delta) is varied in the range from *T*=0.1*s* to *T*=5.0*s* with an increment of 0.1*s*, and the viscous damping coefficient ζ is 5%.

Table 1: Deterioration parameter

Acronym	Deterioration type	Λ_S	Λ_A	Λ_K	c_S, c_A, c_K	$D^{+/-}$
*D*1	no	∞	∞	∞	1.0	1.0
*D*2	slow	100	100	200	1.0	1.0
*D*3	medium	50	50	100	1.0	1.0
*D*4	rapid	25	25	50	1.0	1.0

2.5 Seismic collapse capacity

According to [1] the collapse capacity is defined as the maximum ground motion intensity at which a structure still maintains dynamic stability. If this intensity is infinitesimally increased, the response quantity (here φ) grows unbounded. There is no unique definition of the measure of intensity of seismic excitation. In modern earthquake engineering, however, the most common intensity measure is the 5% damped spectral pseudo-acceleration, $S_a(T, \zeta = 0.05)$, at the elastic period *T* of the considered structure.

In the present study the relative collapse capacity, which is based on this intensity measure, i.e. [11]

$$CC_l = \left. \frac{S_{a,l}}{g\gamma} \right|_{collapse} \tag{5}$$

is utilized. In this equation *g* denotes the gravity acceleration, and $\gamma = f_y / (mg)$ is the yield strength coefficient, defined as the ratio of the yield strength, $f_y = M_{sy} / h$, to the total weight, mg, of the SDOF system. The relative collapse capacity CC_l depends strongly on the underlying ground motion record specified by index *l*. In the present study the record-to-record variability of the collapse capacity is captured through the 44 ordinary ground motions compiled in the far-field set of the FEMA P-695 report [16] referred to as FEMA P-695-FF set. Shome and Cornell [17] provide good arguments that the seismic record-dependent collapse capacities are log-normally distributed. This has been confirmed in [6] and [8] for P-delta sensitive structures. A log-normal distribution is characterized by a measure for central tendency (μ) and a measure for dispersion (σ) [18]. These two quantities are related to the median, 16th and 84th percentiles (referred to as CC, CC^{P16}, and CC^{P84}, respectively) of the individual record-depending collapse capacities CC_l ($l = 1, ..., 44$) as [18]:

$$s^* = \sqrt{\frac{CC^{P84}}{CC^{P16}}} \quad , \quad \sigma = \ln s^* \quad , \quad \mu = \ln CC \tag{6}$$

Here, incremental dynamic analysis (IDA) [19] is used to determine the collapse capacity of an SDOF system with a certain set of assigned structural parameters. In this analysis non-linear response history analyses are performed for a specific earthquake record incrementing its intensity repeatedly up to collapse. For each intensity level the relative intensity $S_{a,l} / g / \gamma$ is plotted against the characteristic peak displacement parameter $\max|\varphi| / \varphi_y$, resulting in the IDA curve. Collapse is attained, when either the deformation ratio $|\varphi| / \varphi_y$ grows to infinity due to second order effects, or the spring deteriorates until it cannot resist any excitation anymore. In the analysis the latter collapse criterion is checked by evaluating the spring restoring moment M_S. As an example, in Fig. 4a an IDA curve of an SDOF system up to collapse is depicted.

2.6 Collapse capacity spectra

The representation of the seismic collapse capacity of a non-material deteriorating SDOF system vulnerable to P-delta with assigned damping parameter ζ, negative post-yield stiffness ratio $\theta - \alpha$, and hysteretic loop as a function of the elastic structural period T is referred to as collapse capacity spectrum [6]. As an example, Fig. 4b shows for a system with bilinear hysteretic loop, a negative post-yield stiffness ratio $\theta - \alpha$ of 0.10, and viscous damping ζ of 0.05 the collapse capacity spectrum for record DU99bo2 of the FEMA P695-FF set. Adam and Jäger [6, 7] established median collapse capacity spectra for a large range of characteristic structural parameters based on an extensive parametric study using several sets of earthquake records.

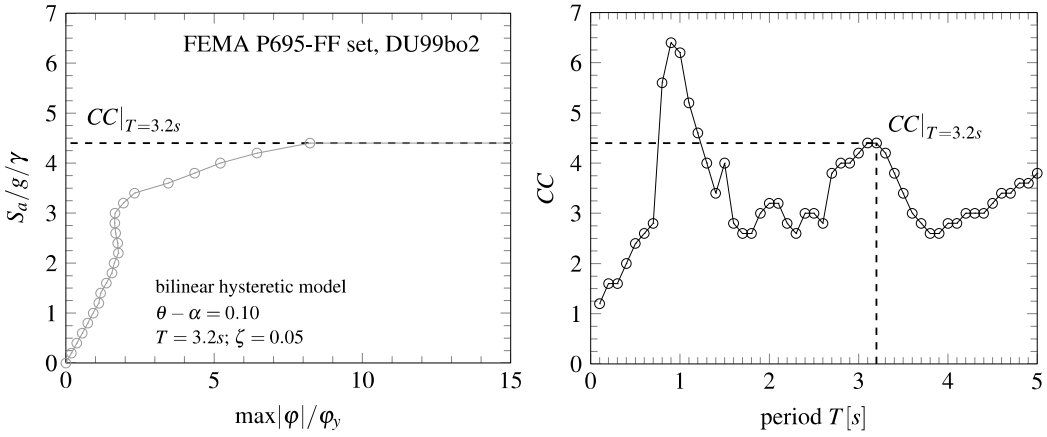

(a) (b)

Figure 4. (a) IDA curve and (b) collapse capacity spectrum for a single earthquake record

3. COLLAPSE CAPACITY SPECTRA FOR SYSTEMS EXHIBITING BILINEAR HYSTERETIC BEHAVIOR

Subsequently, median collapse capacity spectra and collapse dispersion spectra for bilinear SDOF systems with various parameter configurations are assessed with respect to their vulnerability to material deterioration, and they are set in contrast with the outcomes of the base case defined in [6]. Ratios of collapse capacities are determined, where the denominator is the collapse capacity of the base case. If such a ratio is less than one, the collapse capacity of the considered SDOF configuration is smaller compared to the base case. Otherwise, a ratio larger than one indicates that the actual SDOF system is statistically less vulnerable to dynamic instability [6].

3.1 Base case: P-delta effect, no material deterioration, bilinear hysteretic behavior

Fig. 5a shows median collapse capacity spectra for non-deteriorating P-delta sensitive 5% damped SDOF systems with bilinear cyclic behavior, based on the 44 records of the FEMA P695-FF set. Each graph refers to a specific negative slope of the negative post-yield stiffness ratio $\theta-\alpha$. In particular, results for $\theta-\alpha$=0.03, 0.04, 0.06, 0.10, 0.20 and 0.40 are depicted. In [6] and [13] these spectra are considered as base case, denoted as $CC_{P50}\big|_{\text{base case}}$. Since for this base case material deterioration is not present, collapse may only occur due to P-delta, i.e., the post-yield stiffness ratio is larger than 0: $\theta-\alpha$>0. As already discussed in detail in [6], naturally, for fixed structural period *T* the collapse capacity decreases with increasing negative slope of the post-yield stiffness ratio $\theta-\alpha$. Fig. 5b shows the corresponding spectra for the dispersion parameter σ, Eq. (6). σ is an appropriate measure of the record-to-record variability of the collapse capacity. According to these outcomes σ is small for very stiffness systems [7] and is in average about 0.45 for higher periods. Systems with larger $\theta-\alpha$ values fail more likely, and consequently the dispersion is smaller.

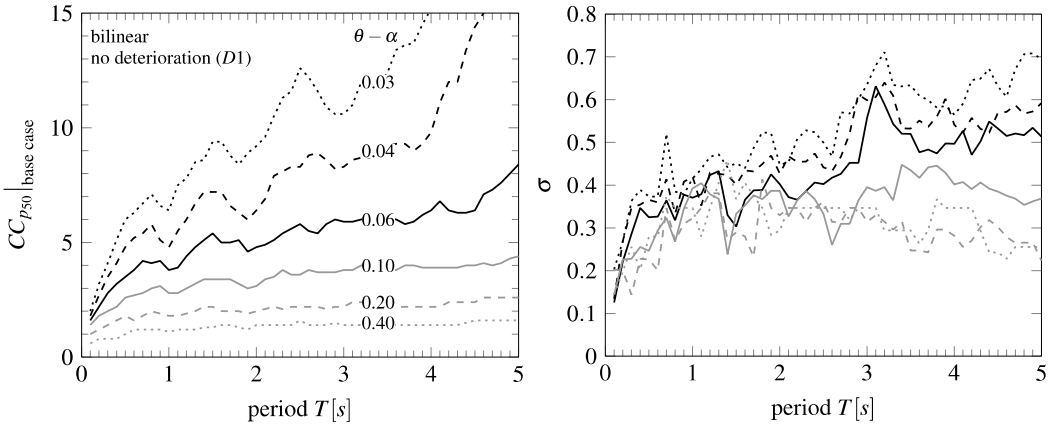

(a) (b)

Figure 5. Base case: (a) Median collapse capacity spectra, and (b) dispersion spectra for P-delta sensitive systems exhibiting non-deteriorating bilinear cyclic behavior (after [6])

3.2 P-delta effect, material deterioration, bilinear hysteretic behavior

Combined cyclic strength and stiffness deterioration with parameters as listed in Table 1 is taken into account. All other parameters comply with the ones of the base case, i.e. bilinear cyclic behavior, and negative slope of the post-yield stiffness ratio. The resulting median and dispersion collapse capacity spectra are shown in Figs. 6 (slow deterioration), 7 (medium deterioration) and 8 (rapid deterioration). It is readily observed that compared to the base case the relative collapse capacities decrease with increasing deterioration speed. For SDOF systems with small $\theta-\alpha$ values (up to 0.06) the impact of material deterioration is more pronounced than for SDOF systems with negative post-yield stiffness ratios $\theta-\alpha \geq 0.10$. It is interesting to note that for small negative post-yield stiffness ratios $\theta-\alpha$ and long-period systems the dispersion is smaller compared to the base case, see Fig. 5b and Figs. 6b, 7b and 8b. I.e., the consideration of material deterioration leads to a decrease of the RTR variability of the collapse capacity. The deterioration speed itself has only a minor impact on the collapse variability.

The effect of material deterioration is quantified in Fig. 9, where the ratio of the median collapse capacity considering material deterioration with respect to the base case is depicted. This figure shows that *slow* material deterioration has only a minor impact on the collapse capacity, even when the negative post-yield stiffness ratio $\theta-\alpha$ is small (i.e., 0.03, 0.04), in particular for stiff systems. Furthermore, it is readily seen that with increasing period *T* the influence of material deterioration becomes more important. For example, for $\theta-\alpha$=0.03 at period *T*=5.0*s* the reduction of the relative collapse capacity is more than 40% compared to the corresponding base case, whereas at period *T*=1.0*s* the reduction is about 10% only. As long as the post-yield ratio stays small ($\theta-\alpha$=0.03 to $\theta-\alpha$=0.06), the defied deterioration speed decreases the resulting collapse capacity with increasing deterioration speed. However, the relative collapse capacity of P-delta sensitive SDOF systems exhibiting a larger negative post-yield stiffness ratio ($\theta-\alpha$>0.06) is not significantly influenced by material deterioration, independently from the deterioration speed.

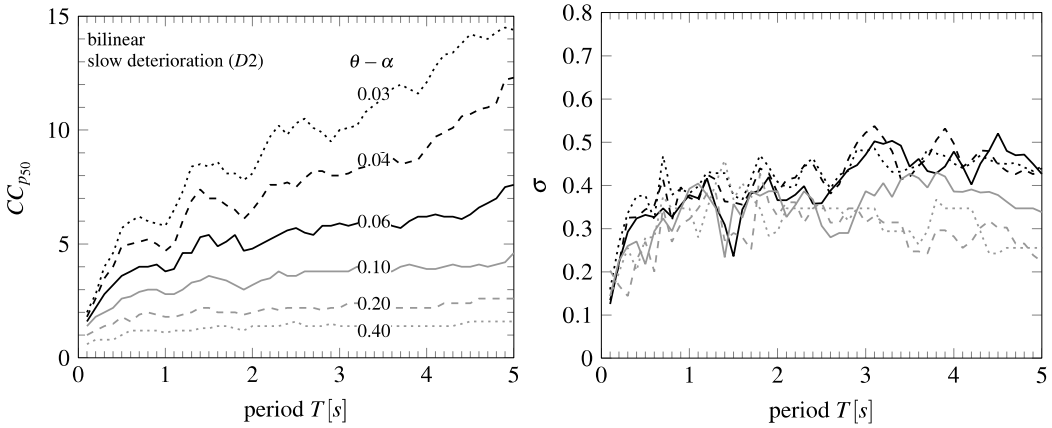

Figure 6. (a) Median collapse capacity spectra, and (b) dispersion spectra for P-delta sensitive systems exhibiting slow deteriorating bilinear cyclic behavior

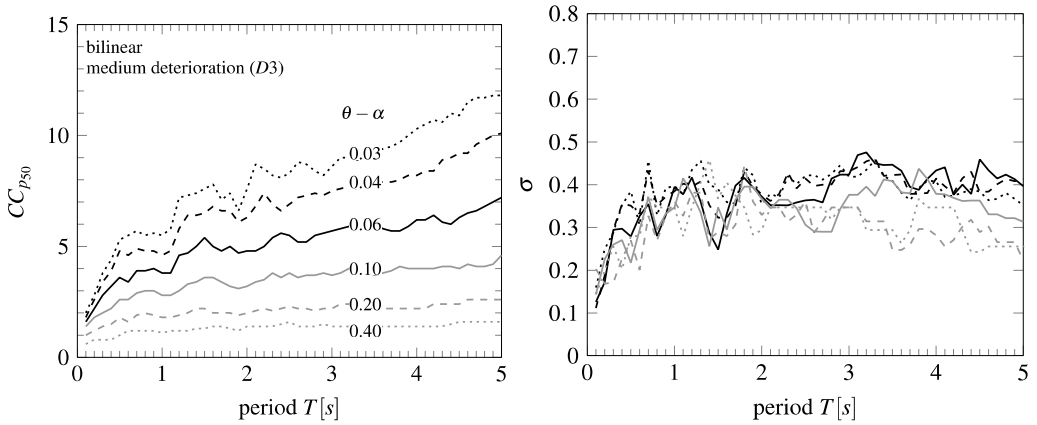

Figure 7. (a) Median collapse capacity spectra, and (b) dispersion spectra for P-delta sensitive systems exhibiting medium deteriorating bilinear cyclic behavior

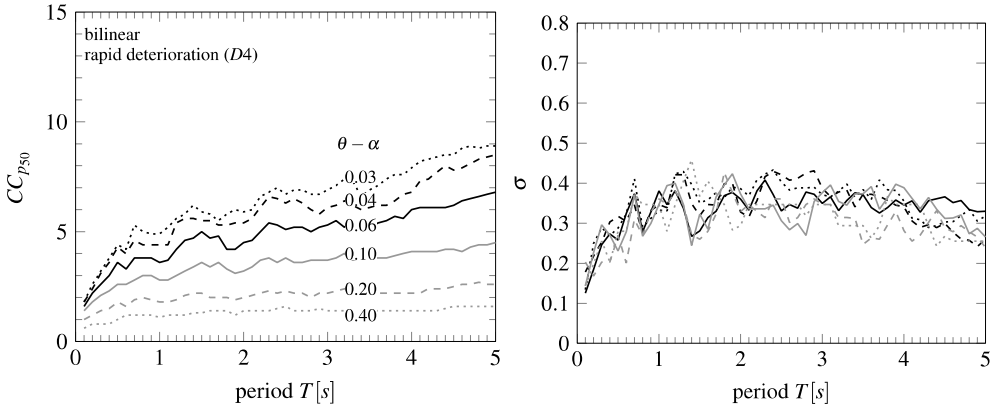

Figure 8. (a) Median collapse capacity spectra, and (b) dispersion spectra for P-delta sensitive systems exhibiting rapid deteriorating bilinear cyclic behavior

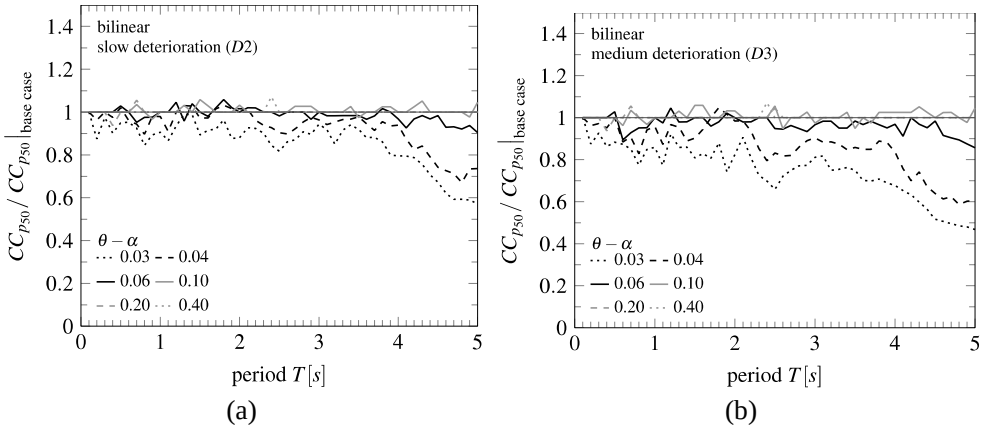

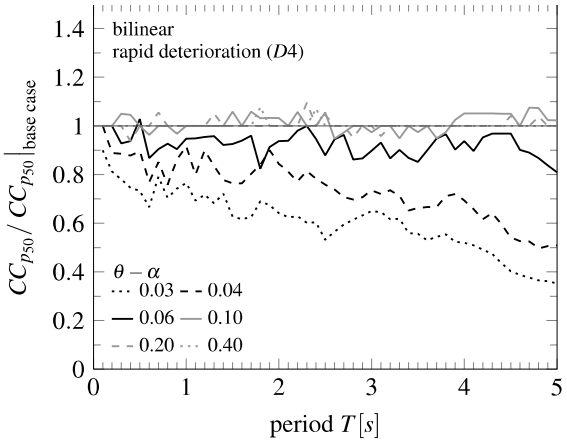

(c)

Figure 9. Median collapse capacity ratios with respect to the base case for P-delta sensitive systems exhibiting deteriorating bilinear cyclic behavior: (a) slow, (b) medium, and (c) rapid deterioration

3.3 No P-delta effect, material deterioration, bilinear hysteretic behavior

For a better understanding of the influence of material deterioration on the collapse capacity, the destabilizing effect due to gravity loads is neglected. Thus, collapse is a consequence of material deterioration only. Median and dispersion collapse capacity spectra derived for bilinear systems with deterioration parameters as defined in Table 1 are depicted in Fig. 10.

For the sake of comparison, in Fig. 10a additionally outcomes of the base case study with negative post yield stiffness ratios $\theta - \alpha$ of 0.03 and 0.04, respectively, are also depicted. Note that the outcomes of P-delta vulnerable systems and systems vulnerable to material deterioration cannot be compared directly, because for the former systems the results are shown for specific $\theta - \alpha$ values, which is not possible for P-delta insensitive systems. It is, however, observed that up to a period of T=4.0s the relative collapse capacities for systems exhibiting rapid material deterioration are almost identical to the ones of the base case with a negative post-yield stiffness ratio $\theta - \alpha$=0.04. For larger periods the relative collapse capacity is smaller for rapidly deteriorating systems. Naturally, an increase of the material deterioration speed reduces the relative collapse capacity significantly. For instance, at a period of T=5.0s the collapse capacity of the system with medium deterioration is about 50% of the case with slow deterioration.

In the medium-period range the dispersion is significantly larger compared to P-delta vulnerable systems, compare Fig. 10b with Fig. 5b. As shown in Fig. 10b, the RTR variability of the collapse capacity becomes in the entire period range slightly smaller when the deterioration speed increases.

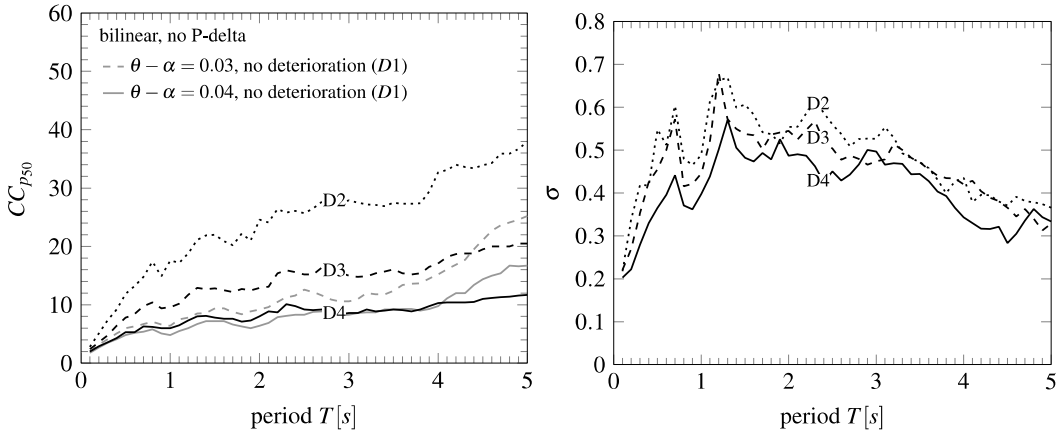

(a) (b)

Figure 10. (a) Median collapse capacity spectra, and (b) dispersion spectra for systems exhibiting slow, medium, and rapid deteriorating, respectively, cyclic bilinear behavior (no P-delta)

4. COLLAPSE CAPACITY SPECTRA FOR SYSTEMS EXHIBITING PEAK-ORIENTED HYSTERETIC BEHAVIOR

Here, median collapse capacity spectra and dispersion spectra are assessed based on the same parameter set as in the previous studies. Instead of a bilinear hysteretic rule, however, a peak hysteretic model is assigned to the SDOF systems.

4.1 P-delta effect, no material deterioration, peak-oriented hysteretic behavior

Median and dispersion spectra for this parameter configuration, originally presented in [6], are depicted in Fig. 11. Fig. 12 shows the ratio of the median spectra to the corresponding base case median spectra of Fig. 5a. Since for all $\theta - \alpha$ values the ratio is in the almost entire period range larger than one it can be concluded that SDOF systems exhibiting bilinear hysteretic behavior are more vulnerable to P-delta than systems with assigned peak-oriented (or pinching) hysteretic model (Fig. 12). I.e., bilinear SDOF systems collapse at a lower seismic intensity. This observation is consistent with results from [14], [11] and [6]. Comparison of Figs. 11b and Fig. 5b reveals that the collapse dispersion is of the same magnitude as for bilinear cyclic systems vulnerable to P-delta.

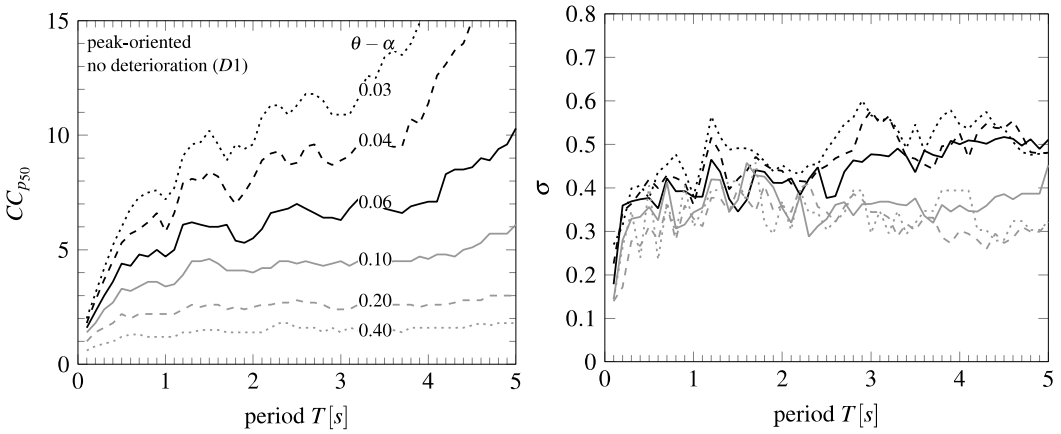

Figure 11. (a) Median collapse capacity spectra, and (b) dispersion spectra for P-delta sensitive systems exhibiting non-deteriorating peak-oriented cyclic behavior

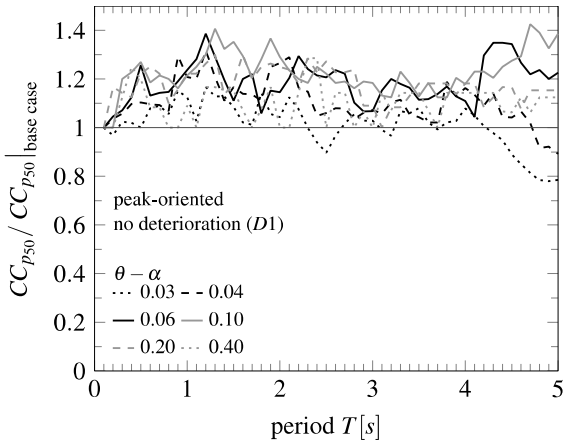

Figure 12. Median collapse capacity ratios for P-delta sensitive systems exhibiting non-deteriorating peak-oriented cyclic behavior with respect to the base case exhibiting bilinear cyclic behavior

4.2 P-delta effect, material deterioration, peak-oriented hysteretic behavior

Median and dispersion collapse capacity spectra based on a peak-oriented hysteretic law exhibiting material deterioration and considering second order effects are shown in Figs. 13, 14 and 15. As already revealed for bilinear systems, a small negative post-yield stiffness ratio is related to a distinct vulnerability of the system to material deterioration. However, for values $\theta - \alpha \geq 0.10$ collapse is governed by P-delta only, since these systems exhibit a smaller number of hysteretic cycles (combined with cyclic deterioration) before they collapse. Naturally, compared to the situation without material deterioration, for rapid material deterioration the reduction of the collapse capacity is more pronounced. Comparing the median collapse capacity spectra of Fig. 6 to 8 and Figs. 13 to 15 reveals that for combined P-delta and material deterioration sensitive structures the underlying hysteretic model has a minor impact on the collapse capacity of SDOF systems exhibiting rapid

material deterioration and small $\theta - \alpha$ values (i.e., $\theta - \alpha < 0.10$). The dispersion of bilinear and peak-oriented deteriorating SDOF systems is of the same order.

Fig. 16 shows collapse capacity ratios with respect to the base case. Depending on the actual $\theta - \alpha$ value the collapse capacity is larger ($\theta - \alpha \geq 0.10$) or smaller ($\theta - \alpha \leq 0.06$) compared to the base case.

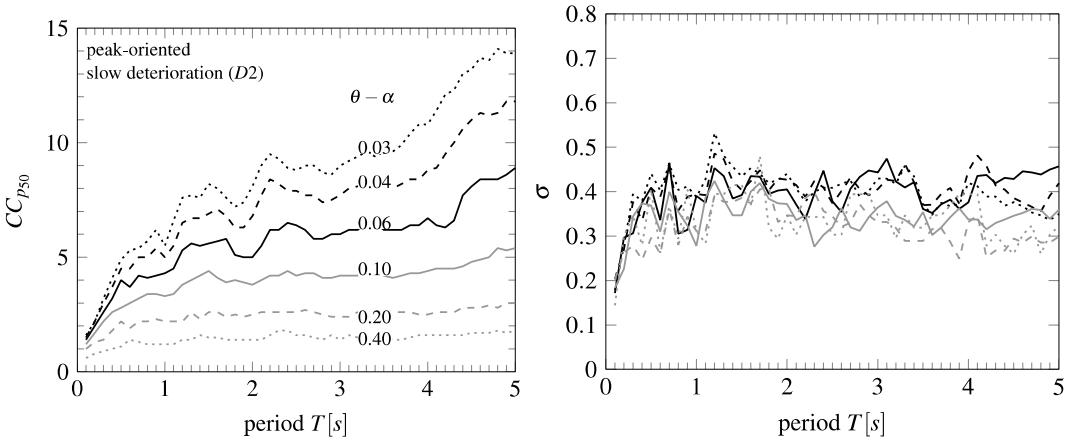

(a) (b)

Figure 13. (a) Median collapse capacity spectra, and (b) dispersion spectra for P-delta sensitive systems exhibiting slow deteriorating peak-oriented cyclic behavior

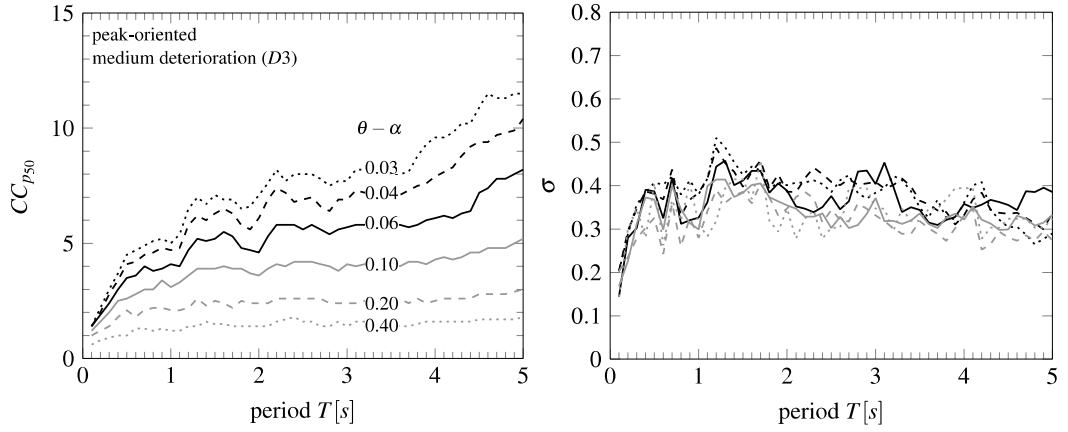

(a) (b)

Figure 14. (a) Median collapse capacity spectra, and (b) dispersion spectra for P-delta sensitive systems exhibiting medium deteriorating peak-oriented cyclic behavior

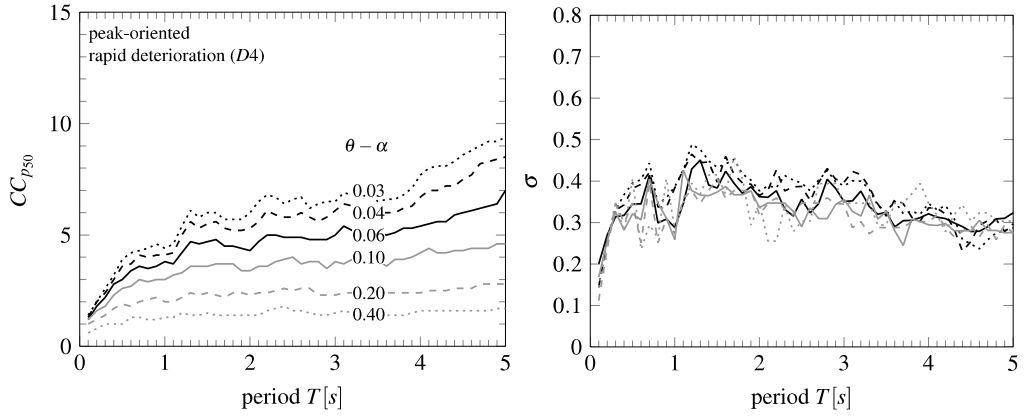

Figure 15. (a) Median collapse capacity spectra, and (b) dispersion spectra for P-delta sensitive systems exhibiting rapid deteriorating peak-oriented cyclic behavior

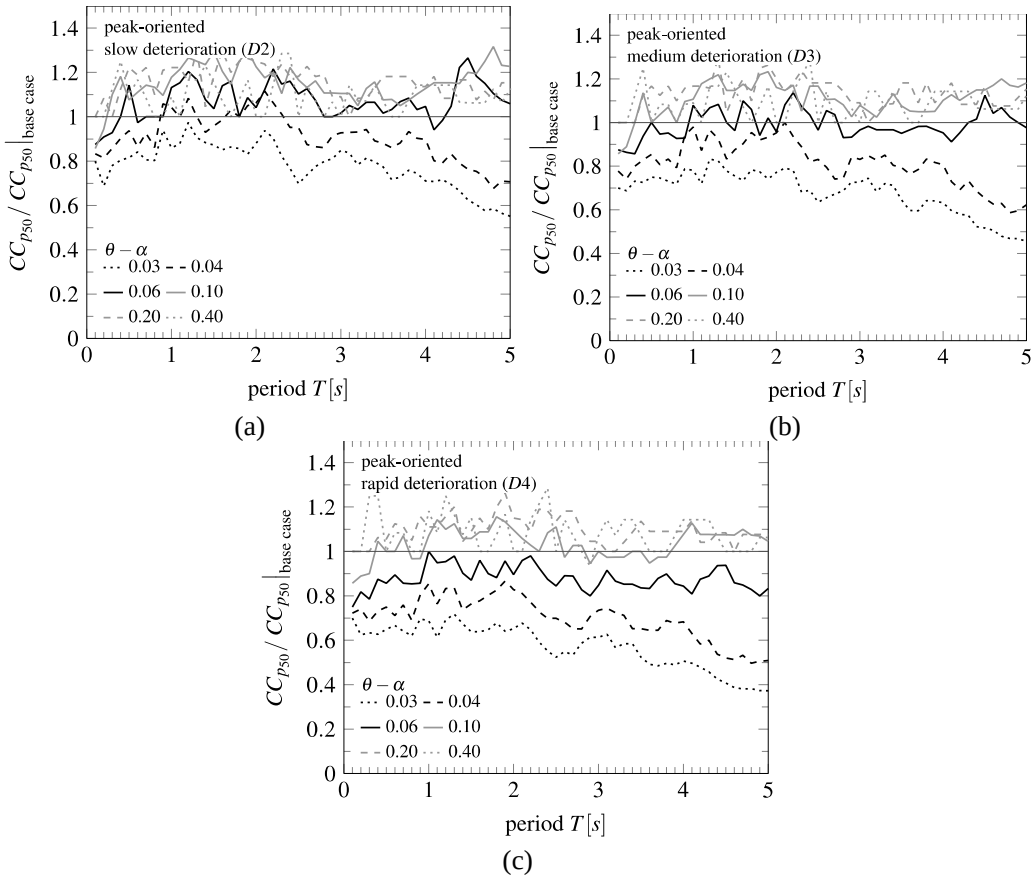

Figure 16. Median collapse capacity ratios with respect to the base case for P-delta sensitive systems exhibiting deteriorating peak-oriented cyclic behavior: (a) slow, (b) medium, and (c) rapid deterioration

4.3 No P-delta effect, material deterioration, peak-oriented hysteretic behavior

Comparing Fig. 17a with Fig. 10a shows that for pure material deterioration, systems with peak-oriented cyclic behavior exhibit a much larger collapse capacity compared to bilinear systems. For slow material deterioration (D2) the difference in the median collapse capacities is about 40%. This is a completely different collapse behavior compared to systems with combined material deterioration and P-delta, where for large $\theta - \alpha$ values the median collapse capacities are almost unaffected by the underlying hysteretic law, see Fig. 9 and Fig. 16. Furthermore, it seems that P-delta has a larger effect on systems with peak-oriented cyclic behavior, because the collapse capacity difference between P-delta sensitive systems only (dashed lines in Fig. 17a) and material sensitive systems only (solid lines in Fig. 17a) is much larger compared to bilinear systems (Fig. 10a). The magnitude of the RTR collapse capacity dispersion is in the entire period range about the same as for bilinear deteriorating systems, see Figs. 17b and 10b.

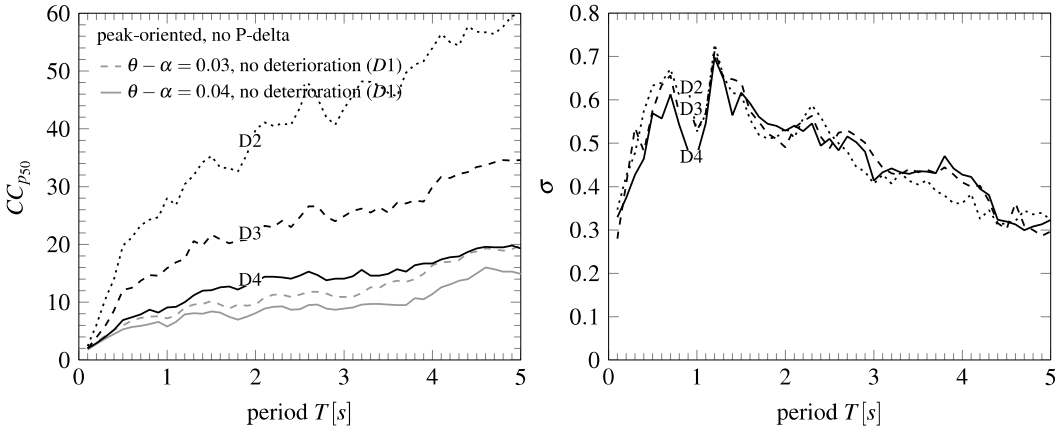

(a) (b)

Figure 17. (a) Median collapse capacity spectra, and (b) dispersion spectra for systems exhibiting slow, medium, and rapid deteriorating, respectively, cyclic peak-oriented behavior (no P-delta)

5. SUMMARY AND CONCLUSIONS

In a fundamental parametric study the vulnerability of seismic excited inelastic deteriorating single- degree-of-freedom (SDOF) systems to dynamic instabilities has been examined. Focus has been on the assessment of the relative collapse capacity, defined as the ratio of the 5% damped spectral acceleration at the structural period to a strength parameter. In particular, the impact of P-delta, material deterioration, and hysteretic modeling has been quantified.

From the outcomes of this study it can be concluded that for the considered systems in general second order effects affect more the relative median collapse capacity than material deterioration. Neither the assigned hysteretic cyclic model nor material deterioration has a significant impact on the collapse capacity if the difference of stability coefficient θ and

hardening ratio α is larger than 0.20 (i.e., these systems are significantly prone to P-delta induced collapse). Bilinear SDOF systems are more vulnerable to P-delta induced collapse than systems with peak-oriented or pinching hysteretic model, independently of the deterioration speed. In contrast, if the negative post-yield stiffness ratio is small, i.e. $\theta - \alpha \leq 0.06$, the effect of material deterioration on the seismic collapse capacity cannot be disregarded. For long period systems ($T \geq 4.0$s) and *rapid* material deterioration the median collapse capacity is up to 50% smaller, compared to the case considering P-delta only. Also for *slow* deterioration a reduction of 80% is observed. From the derived results it can be concluded that combined material deterioration and P-delta reduces significantly the relative collapse capacity of long period systems, which exhibit *rapid* material deterioration and a small P-delta induced negative post-yield stiffness ratio. Thus, for those systems collapse capacity spectra considering P-delta only [6] cannot be used for a reliable simplified assessment of the seismic collapse capacity according to the collapse capacity spectrum methodology.

REFERENCES

1. Krawinkler H, Zareian F, Lignos D, Ibarra LF. Prediction of collapse of structures under earthquake excitations, *Proceedings of the 2nd International Conference on Computational Methods in Structural Dynamics and Earthquake Engineering (COMPDYN 2009)*, Papadrakakis M, Lagaros ND, Fragiadakis M (eds), June 22-24. Rhodes, Greece, 2009, CD-ROM paper, Paper No. CD449, 19 p.
2. Adam C, Ibarra LF, Krawinkler H. Evaluation of P-delta effects in non-deteriorating MDOF structures from equivalent SDOF systems, *Proceedings of the 13th World Conference on Earthquake Engineering (13WCEE)*, August 1-6, Vancouver BC, Canada, DVD-ROM paper, 2004, 15 p.
3. Lignos D, Krawinkler H. Deterioration modeling of steel components in support of collapse prediction of steel moment frames under earthquake loading, *Journal of Structural Engineering*, **137**(2011) 1291-302.
4. Lignos D, Krawinkler H, Whittaker AS. Prediction and validation of sidesway collapse of two scale models of a 4-story steel moment frame, *Earthquake Engineering and Structural Dynamics*, **40**(2011) 807-25.
5. Lignos D, Sidesway collapse of deteriorating structural systems under seismic excitations, PhD thesis, Stanford University, Department of Civil and Environmental Engineering, 2008.
6. Adam C, Jäger C. Seismic collapse capacity of basic inelastic structures vulnerable to the P-delta effect, *Earthquake Engineering and Structural Dynamics*, **41**(2012) 775-93.
7. Jäger C, Adam C. Influence coefficients for collapse capacity spectra, *Journal of Earthquake Engineering*, **17**(2013) 859-78.
8. Adam C, Jäger C. Simplified collapse capacity assessment of earthquake excited regular frame structures vulnerable to P-delta, *Engineering Structures*, **44**(2012) 159-73.

9. Adam C, Krawinkler H. Large displacement effects on seismically excited elastic-plastic frame structures, *Asian Journal of Civil Engineering*, **5**(2004), 41-55.
10. Medina RA, Krawinkler H. Seismic demands for nondeteriorating frame structures and their dependence on ground motions, Report No. 144, The John A. Blume Earthquake Engineering Research Center, Department of Civil and Environmental Engineering, Stanford University, Stanford, CA, 2003.
11. Ibarra LF, Krawinkler H. Global collapse of frame structures under seismic excitations, Report No. PEER 2005/06, Pacific Earthquake Engineering Research Center, University of California, Berkeley, CA, 2005.
12. Ibarra LF, Medina RA, Krawinkler H. Hysteretic models that incorporate strength and stiffness deterioration, *Earthquake Engineering and Structural Dynamics*, **34**(2005) 1489-511.
13. Jäger C. The collapse capacity spectrum method. A methodology for rapid assessment of the collapse capacity of inelastic frame structures vulnerable to P-delta subjected to earthquake excitation (in German), PhD thesis, University of Innsbruck, 2012.
14. Rahnama M, Krawinkler H. Effect of Soft Soils and Hysteresis Model on Seismic Demands, Report No. 108, The John A. Blume Earthquake Engineering Research Center, Department of Civil and Environmental Engineering, Stanford University, Stanford, CA, 1993.
15. MacRae GA. P-Delta effects on single-degree-of-freedom structures in earthquakes, *Earthquake Spectra*, **10**(1994). 539-68.
16. FEMA P-695. *Quantification of Building Seismic Performance Factors*, Federal Emergency Management Agency, Washington DC, 2009.
17. Shome N, Cornell CA. Probabilistic seismic demand analysis of nonlinear structures, RMS Tech Report No. 38, The John A. Blume Earthquake Engineering Research Center, Department of Civil and Environmental Engineering, Stanford University, Stanford, CA, 1999.
18. Limpert E, Stahel WA, Abbt M. Log-normal distributions across the sciences: keys and clues, *BioScience*, **51**(2001) 341-52.
19. Vamvatsikos D, Cornell CA. Incremental dynamic analysis, *Earthquake Engineering and Structural Dynamics*, **31**(2002) 491-514.